

# NEW APPROACH FOR AUTOMATIC DETECTION OF BUILDINGS IN AIRBORNE LASER SCANNER DATA USING FIRST ECHO ONLY

F. Tarsha-Kurdi, T. Landes\*, P. Grussenmeyer, E. Smigiel

Photogrammetry and Geomatics Group, MAP-PAGE UMR 694 - INSA de Strasbourg, 67000 Strasbourg, France  
(fayez.tarshakurdi|tania.landes|pierre.grussenmeyer|eddie.smigiel@insa-strasbourg.fr)

Commission III, WG III/3

**KEY WORDS:** LIDAR, Urban, Processing, Detection, Building, Segmentation, Classification

## ABSTRACT:

Airborne laser scanning has become a significant 3D data acquisition technique in the field of surveying. By measuring point clouds defined in three-dimensional coordinates, this technique provides almost automatically Digital Surface Models (DSMs). But for 3D city modelling, the discrimination between terrain and elevated objects based on this surface model is still a challenging task, since fully automatic extractions are not operational. Moreover, some of the available methods combine several echoes although echo separation is not always obvious and sometimes last echo is not reliable. In this context, the aim of this study is to develop a general automatic segmentation method of Lidar point clouds focussing exclusively on the first echo and without any external data. The result of the proposed methodology is the automatic discrimination of the buildings and the terrain, by excluding vegetated areas. In the first step, terrain and off-terrain clouds are discriminated, based mainly on threshold features as proposed in the literature, but improved and generalized to the case of brutal terrain discontinuities. In the second step, buildings and vegetation are categorized as subclasses of the off-terrain class. The innovation of the exposed approach lies in the exploitation of the whole analysis levels combining points, pixel, segment and spatial information. Thus, the processing chain fully benefits from the planimetric and altimetric information of a point cloud. The complete workflow is presented, as well as its limitations. At last, the satisfying results obtained for three different test sites covered by two cloud densities validate our processing chain.

## 1. INTRODUCTION

### 1.1. Motivation and goals

Most GIS applications need digital terrain models (DTMs) or digital 3D building models as reference layers for subsequent processes. Automatic extraction of man-made objects, particularly 3D building models is a coveted topic (Baltsavias et al., 2001). Currently available DTMs or DEMs covering wide areas come rather from the processing of stereo pairs acquired by optical or radar satellite sensors. Nevertheless, the resolution and accuracy of derived products do not yet match the requirement standards in urban surveying. This is why, before the Lidar technology, photogrammetric techniques applied to aerial photos were the best issue.

The suitability of airborne laser scanning techniques for 3D object reconstruction has been proved over the last decade (Maas, 2005). Nevertheless, although DTM as well as building models are inherent to DSMs, their extraction was never completely or automatically carried out. When using multiple and reliable echoes, results are often very satisfying (Wotruba et al., 2005), since the second echo helps to distinguish points captured on the top of the canopy from those captured on the ground. But in most cases, either the second echo is less accurate than the first one (Yu et al., 2005) or it is not always separable from the first one (Pfeifer et al., 1999; Wotruba et al., 2005).

In this context, the goal of present project is to develop a general segmentation method for the automatic extraction of buildings using the first echo only.

### 1.2. Related work

The first goal in the processing of laser scanning data is the segmentation of acquired points into terrain and off-terrain

classes. In this paper, segmentation means an extraction of point clusters describing a specific class. As summarized in (Maas and Vosselman, 1999), such segmentation may be obtained using additional sources of data, such as 2D GIS information or reflectance information; other processes analyse the local histograms or use filtering techniques considering exclusively Lidar data. Despite the difficulty to categorize complex processes, the latter family could be subdivided into: (a) approaches where the support is mainly an image produced by interpolation and/or segmentation. In this case, segmentation means mainly generation of objects composed of similar pixels; (b) approaches trying to concentrate processing on point level and where segmentation means the discrimination of several clusters in a point cloud. In the category (a), digital image processing techniques are employed, e.g. remote sensing classification methods (Maas, 1999; Tóvári and Vögtle, 2004; Lohmann and Jacobsen, 2004); digital filters related to morphological filtering methods (Lohmann et al., 2000; Vosselman, 2000; Sithole, 2001) or to Fast Fourier Transformations (Marmol and Jachimski, 2004); theory of active shape models (Elmqvist, 2001; Weinacker et al., 2004). In the category (b), the procedures try to stay or return at the Lidar point cloud level, sometimes in an iterative way. One can cite the use of interpolation methods such as the linear prediction method (Kraus and Pfeifer, 1998; Rottensteiner and Bries, 2002), the 3D surface detection (Lee and Schenk, 2002) or the octree structure based segmentation (Whang and Tseng, 2004).

### 1.3. Position of proposed approach

For the first segmentation of terrain and off-terrain points, the algorithm developed in this paper finds its place in the category (a), because a raster DSM and image processing procedures are

used. Reasons explaining this choice are on the one hand the high computing time required when processing the cloud on a point level with adaptative methods, and on the other hand, the availability of well-known digital image processing functions. Thus, based on the analysis of height features on a previously interpolated DSM, successive operations such as thresholding, gradient and morphological filtering on height features are achieved. Results are improved in order to make the proposed procedure reliable even in steep and discontinuous terrains.

The second segmentation chain performs a discrimination of the off-terrain points into two classes: buildings and vegetation. Our solution joins the category (b) in the sense that it uses the relevant information provided by the original Lidar 3D points. Using jointly the DSM and the initial point cloud, the presented algorithm exploits the fact that one cell or pixel in a DSM may contain one or more points of the cloud. Considering building characteristics, this observation leads to the generation of features, which are specific to buildings and based on 3D topological information. Thus, a large part of vegetation can be removed and buildings can be isolated properly. In this way, proposed approach combines three levels of analysis usually used separately: processing based on a pixel level (Maas, 1999; Rottensteiner and Briese, 2002), processing based on a segment level (Lohmann and Jacobsen, 2004; Tóvári and Vögtle, 2004) and that based on a spatial level (Wang and Tseng, 2004).

## 2. DATA

In order to test our approach on different point densities, two types of data covering three areas are used (Table 1).

Test sites	“Hermann”	“Victoire boulevard”/ “Strasbourg centre”
Acquisition	End of June 2002	Begin September 2004
Sensor	TopoEye	TopScan (Optech ALTM 1225)
Points density	7-9 points / m <sup>2</sup>	1.3 points / m <sup>2</sup>
Flight height	200 m	1440 m
Pulse frequency	7 kHz	25 kHz
Field of view	± 20 degrees	±26 degrees
Points/dataset	410 497	450 000 and 400 000

Table 1. Characteristics of the three datasets used in this study

The first test site “Hermann” is a residential area in periphery of Helsinki, where large and spaced storey houses are surrounded by vegetation. This point cloud belongs to the building extraction project of EuroSDR ([www.eurohdr.org](http://www.eurohdr.org)). The second test site called “Victoire boulevard” is located in the campus district of Strasbourg, along a road where trees are near to large buildings. Finally, the third cloud “Strasbourg centre” covers the centre of Strasbourg city, known for its tangled up houses. TopScan has acquired the last two clouds during the same campaign. Unfortunately, only the first echo is reliable.

## 3. WORK FLOW FOR OFF-TERRAIN DETECTION

The first segmentation step consists in separating the off-terrain points (building, vegetation, trees) from the ground. The workflow is presented in the following paragraphs.

### 3.1 Interpolation of a DSM

A Lidar point cloud is represented by 3D points, not always regularly spaced. The use of digital filters requires transforming this dataset into a uniform 2D grid. In order to preserve the real measured altitudes (the fitting surface should follow the Lidar points), a nearest neighbour interpolation technique is used. The well-known advantages of this technique are the low interpolation calculation time and the conservation of the original altitude values. This means, that the topological original relationships between points -in the sense of relative height variations between neighbouring points- can also be preserved by this interpolation. Of course, a determining criterion is the definition of the sampling value (resolution) of the DSM. Under the assumption that the distribution of points is regular and that one pixel must contain at least one point, the average cloud density can be calculated. Thus the sampling interval *SI* can be deduced (1).

$$SI = \frac{1}{\sqrt{\text{density}}} \quad (1)$$

Obviously, the detectable object is directly dependent on the available density, whatever the method of interpolation.

### 3.2 Detection of the off-terrain segment edges

To detect the off-terrain segment edges, as suggested by (Maas, 1999), directional gradient filters are applied on the DSM with 3x3 kernels under eight different rotations ( $k, \pi/4; k=1\dots 8$ ). The first matrix contains value 1 in the upper left cell and value -1 in the lower right cell. Thus, eight bands are generated in which the grey values represent height differences. Then, the maximum gradient for each pixel is searched over the k bands and assigned to a matrix  $\Delta Z$  (equation 2).

$$\Delta Z_{i,j} = \max (G_{i,j})_k \quad (2)$$

where  
*i, j* : pixel position in line and column  
*(G<sub>i,j</sub>)<sub>k</sub>* : k<sup>th</sup> band of filtered image  
*k* : gradient band number ( $k=1, \dots, 8$ )

Comparing the pixel values of the  $\Delta Z$  matrix to a defined threshold  $S_1$ , the detection of the edge pixels is possible. The maximum absolute gradient shows behaviour similar to that of the slope around each pixel. Thus if  $\Delta Z_{i,j} > S_1$  the pixel describes an off-terrain edge (buildings or vegetated area) and takes the value 1 in a binary matrix *A*. The threshold  $S_1$  is defined according to the smallest detectable building. Generally, in the countries we are concerned with, the smallest foreseeable height for a building is 5 to 6 meters. Figure 2a presents the binary matrix *A* obtained for the Hermann test site.

At this stage, two operations occur: the first one consists in filling the body of the off-terrain segment borders already detected. The second one consists, in parallel, in assigning a neighbouring ground value to the off-terrain pixels that facilitates the generation of a DTM.

### 3.3. Detection of the whole off-terrain pixels

In order to fill the body of the segment borders created previously, the neighbourhood of each pixel has to be considered. For this purpose, the matrix *A* and the DSM are analyzed. Firstly, if the central pixel in a 3x3 moving window (moving over *A*) belongs to an edge, the lowest neighbouring altitude is assigned to it (Fig. 3 [1]). Then, the height difference

between the pixel and its neighbours is calculated in matrix  $\Delta Z_{(i,j),(k,l)}$  as expressed in equation 3.

$$\Delta Z_{(i,j),(k,l)} = (Z_{k,l} - Z_{i,j\_ground}) \quad (3)$$

were  $i, j$  : central pixel coordinates  
 $k, l$  : coordinates of the 8 neighbours;  $(k,l) \neq (i, j)$

The moving window takes into account the results obtained by the last position before continuing its progression. This leads to the distinction between the neighbouring pixels in which the altitude has been changed by this step, i.e. projected on the ground  $Z_{k,l\_ground}$  and the neighbouring pixels in which the altitude remains the same, i.e.  $Z_{k,l\_orig}$  (Fig. 3 [2]).

Pixels describing off-terrain objects will present high values for equation 3. Thus, if  $\Delta Z_{(i,j),(k,l)} > S_1$  and simultaneously the neighbouring pixel  $(k,l)$  does not describe an edge in matrix A, the pixel  $(i,j)$  is assigned to the off-terrain class (Fig. 3 [3]) and its altitude becomes  $Z_{i,j\_ground}$ . The threshold  $S_1$  is the same as previously, since maximum height differences are also compared here. Figure 2b presents the resulting binary image.

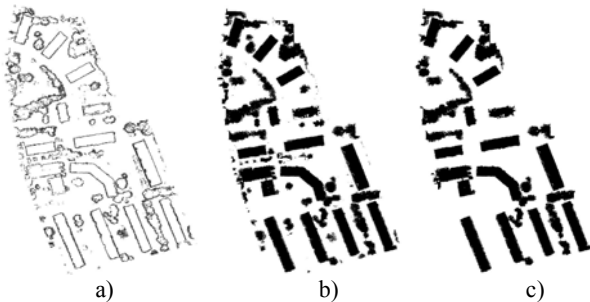


Figure 2. a) Off-terrain segment edges (matrix A). b) Off-terrain class. c) Off-terrain after morphological filtering

### 3.4. Assigning ground altitudes to the off-terrain pixels in a later building extraction purpose

As already mentioned, while off-terrain pixels are assigned to their class, their altitude is replaced, in parallel, by a ground level altitude  $Z_{i,j\_ground}$ . This modification is directly dependent on the surrounding altitude values and on their history ( $Z_{k,l\_ground}$  or  $Z_{k,l\_orig}$ ). So, each off-terrain pixel gets a ground level altitude. Thus, three matrices are output from the workflow summarized in Figure 3: matrix A, the normalized DSM (nDSM) and a matrix called Test\_ground. Matrix A is a binary mask where the off-terrain pixels are non-zero. The nDSM contains the whole pixels belonging to the off-terrain class. The matrix Test\_ground contains three values: 1, 2 and 0. A pixel with a value of 1 means that its altitude in nDSM has been taken from the original dataset; a pixel with value 2 means that its altitude comes from previously modified altitudes, whereas pixels with value 0 belong to the "ground" class (Figure 4). The value 2 occurs generally for pixels located inside the body of the buildings. This is due to the fact, that inside a vegetated area, the laser beam may reach the ground. Whereas this situation is rare in a building segment, except in the case of interior courts. This characteristic (although insufficient) is of crucial importance for the next segmentation step, i.e. for the distinction between buildings and vegetation.

### 3.5. Classification generalization

As suggested by (Vosselman and Maas, 2004), mathematical morphology operations may help to clean the classification from

remaining segment residuals. Two successive operations are applied here. Firstly, a morphological opening allows erasing the punctual segments remaining on the ground. Then, a morphological closing enables filling last gaps occurring in the off-terrain segments (Figure 2c).

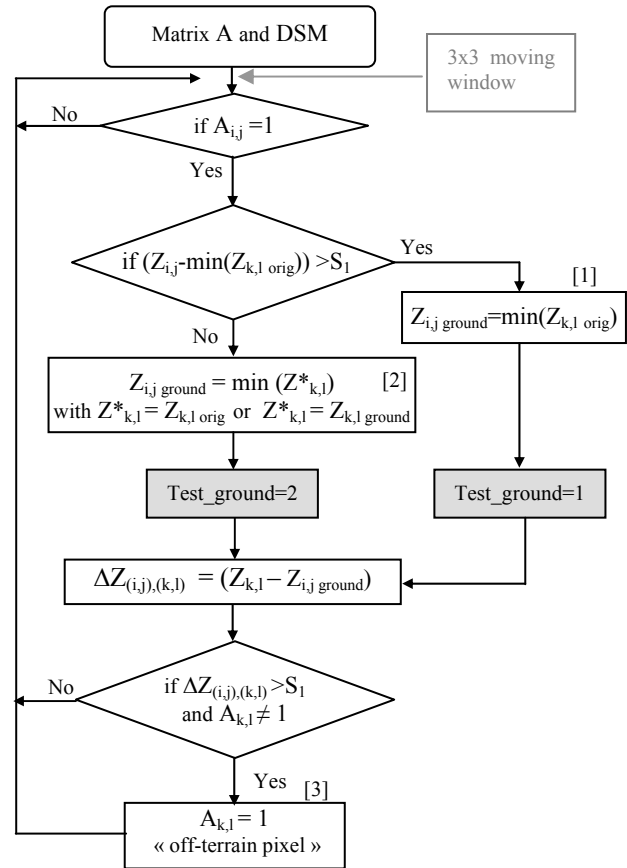


Figure 3. Workflow for the detection of off-terrain pixels

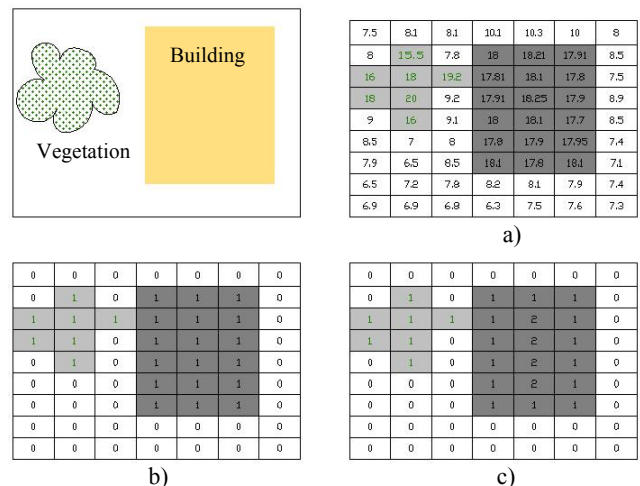


Figure 4. Off-terrain class detection. a) DSM. b) Matrix A. c) Test\_ground matrix.

### 3.6. Improvement of the processing chain to the case of terrain discontinuities

By analysing the results, it becomes clear that the present segmentation based on a sequence of thresholds and

morphological filtering needs improvement in the case of large local terrain discontinuities caused by holes, ditches, noise, etc. Indeed, the cutting surface passes over the terrain surface with a height threshold  $S_1$ . Therefore, in the case of brutal discontinuities, the algorithm misclassifies the pixels behind the ditch as “off-terrain” pixels (Figure 5).

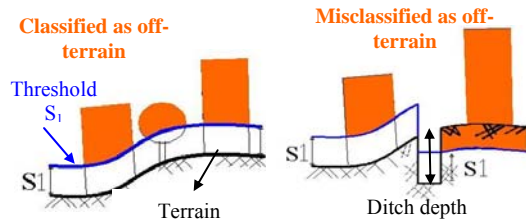


Figure 5. Processing error in the case of terrain discontinuities.

In the case of discontinuities, (Sithole and Vosselman, 2003) showed deficits of all main filtering methods even when the algorithm has some special rules to avoid misclassification next to breaklines. To cope with this problem, we analyzed the reaction of the algorithm on different test sites and in several discontinuities conditions. It becomes clear that the error generated and illustrated in Figure 5 is directly dependent on the direction passage of the mobile matrix. The solution consists simply in achieving the filtering along different directions over the image. The intersection of the intermediate products therefore solves the problem. Figure 6 gives an example. In step (a), the moving window detecting the off-terrain pixels moves over the DSM following the usual and then the opposite direction. It provides detection of the shaded segments in (b) and in (c) respectively, where the lower right part of (b) and the upper left area of (c) are misclassified. The intersection of (b) and (c) cancels the misclassified areas in the step (d). The detected ditch is automatically assigned to the ground class.

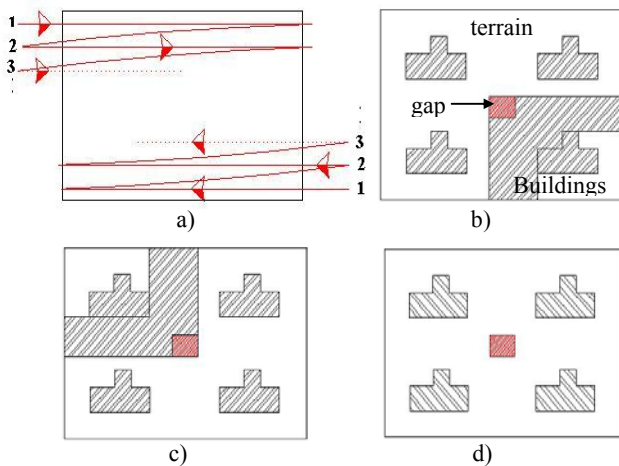


Figure 6. Misclassification correction in the case of terrain discontinuities. a) Moving window movements. b), c) Respective results. d) Ditch cancelling.

By this mean, two classes of points are efficiently generated, i.e. the terrain class (ground) and the off-terrain class (buildings, vegetation, noise, etc.), even in the case of abrupt terrain. The next part will analyse the off-terrain class in order to extract the buildings from it.

#### 4. DETECTION OF BUILDINGS

Various algorithms have been suggested and applied to laser scanning data with the aim of separating buildings from other elevated objects. As mentioned in the introduction, these procedures are mainly based on previously interpolated grids, while often neglecting invaluable information contained in the initial irregular cloud of acquired points.

##### 4.1. Contribution of 3D points contained in one cell

The approach proposed in this paper exploits the fact that one pixel in the nDSM may contain one or more points of the cloud. The 3D position of these cell-points will play an important role in the discrimination procedure of the subclasses vegetation and buildings. Thus, the nDSM and the initial point cloud are used jointly in a pixel level, segment level and spatial analysis level.

Considering one cell, three types of altitude values  $Z$  may occur as illustrated in Figure 7:

1.  $Z_{build}$  : the real topographic altitudes (terrain or off-terrain points);
  2.  $Z_{DSM}$ : the raw DSM values obtained by interpolation of the cloud points;
  3.  $Z_{points}$ : the point altitudes as acquired by the sensor.
- Other interesting features are the extreme values of  $Z$  among the points of a cell ( $min\_Z_{points}$  or  $max\_Z_{points}$ ), etc.

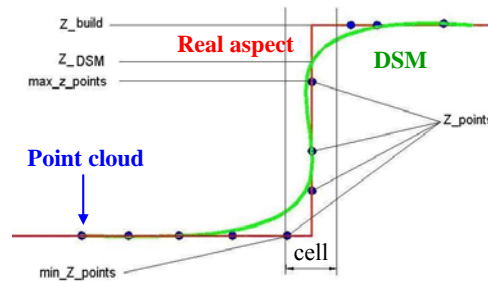


Figure 7. Different types of altitude values occurring in one cell.

##### 4.2. Segmentation methodology developed

The approach for detecting buildings among trees or other objects is based on the assumption that the building roofs are normally composed of flat planes or more generally of surfaces. So, the methodology developed here is based on the search for planes composing the roofs of the buildings, as suggested by (Elaksher and Bethel, 2002). The main advantages lie in the fact that it is possible to adapt the concept to relatively low point densities. Moreover, only the first echo is used and, at last, the segments representing a mixture of buildings and vegetation can be removed.

For the moment, the off-terrain class contains mainly trees and buildings. If we succeed in adjusting a group of points by a plane using the least square method (regarding small residues) a large quantity of points representing vegetation can be eliminated. The implementation of this principle emphasizes limits and constraints. The mathematical detection of the points composing a plane requires a great deal of processing time. Moreover, because of low point density and/or details on the roofs (e.g. chimneys), the distribution of the points on a roof cannot always be adjusted by a plane. Finally, it occurs that vegetation points can be adjusted by an average plane while presenting negligible residues!

To avoid these disadvantages, our approach replaces the mathematical test by topological relationships. As mentioned above, it will benefit from a paramount element in the interpretation of the cloud: the points inside a cell of the DSM. Because of the irregular distribution of Lidar points and the existence of vertical elements, the number of points per pixel in X,Y as well as in Z dimension is variable. So the three topological features we can derive for every cell are:

- The number of points per cell
- The maximum vertical distance between points
- The maximum slope angle of the best fitting plane

These three criterions allow the elaboration of classification rules with the specific aim of building detection. No assumption can easily be made based on the first criterion (number of pixels per cell), since this criterion is very dependant on the point cloud density and regularity. If a cell covers entirely a portion of a roof, then one can put forth the following assumptions:

- Assumption relating to second criterion: the maximum height difference  $\Delta h_{\max}$  between points in a cell will be lower than a certain threshold. The value of the threshold will depend on 3 factors: the sampling of the DSM grid, the roofs geometry (horizontal plane, tilted plan or spherical surface) and the altimetric measurement accuracy.

So  $\Delta h_{\max} = h_2 - h_1$  and if we consider  $\sigma_{h_2} = \sigma_{h_1} = \sigma_h$ , the transmission of errors delivers:  $\sigma_{\Delta h_{\max}} = \sqrt{2} \cdot \sigma_h = \pm 21cm$ , since Lidar data relative accuracy in Z is about  $\pm 15cm$ .

- Assumption relating to third criterion: the maximum slope of a plan adjusting locally a roof is equal to 60 degrees. That allows expressing  $\Delta h_{\max}$  as a function of the sampling interval  $p$  and maximum slope angle, so:  $\tan(60^\circ) = \Delta h / p$ .

Thus, from the last two assumptions we find the threshold of maximum height difference (equation (4)). Under this threshold, the corresponding pixel is assigned to the building class.

$$\Delta h_{\max} \leq \tan(60^\circ) \cdot p + \sqrt{2} \cdot \sigma_h \quad (4)$$

In addition to the last test, the classification rule also takes into account the values 2 representing the body of building segments in the matrix Test\_ground (Figures 3 and 4).

The detected segments represent at first the kernel of building roof planes. In order to complete this kernel with the surrounding pixels, a specific region-growing algorithm has been developed, working on the 8 neighbouring height differences. A last filter erases the remaining segments by regarding the smallest foreseeable building segment. Results obtained through this workflow are very satisfying, since the major part of buildings is well classified. Only a few pixels of vegetation are misclassified and easily rejected by mathematical morphology. Indeed, it happens that a group of points, within the vegetation class, accepts an average plane with negligible residues and respects the whole topological assumptions.

## 5. RESULTS AND DISCUSSION

We applied the proposed algorithm on the three datasets available. The computing time required for extracting buildings is negligible. Figure 9 presents the buildings extracted from the DSM (Figure 8) of the “Victoire boulevard” test site.

In order to evaluate the precision of the building classification, an estimation method suggested by (Sithole and Vosselman, 2003) and based on a confusion matrix has been applied. The classes of interest are “buildings” and “not-buildings”. The

reference images have been conceived by digitizing the buildings in the DSM with the help of aerial images. Three errors characterize the precision of the obtained segmentations and are reported in Table 10. Error I shows the proportion of building-pixels misclassified; Error II the proportion of not-building pixels misclassified and Total Error the proportion of misclassified pixels. The last column presents the mention of the influence of neighbouring points filtering. The different mentions obtained are explained by the different urban typology of the city centre compared to that of areas located in periphery. However, the proposed algorithm provides very good results, for both point densities.

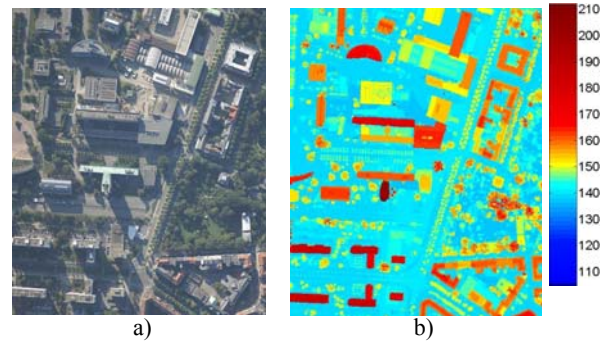


Figure 8. “Victoire boulevard” site. a) Aerial image. b) Pseudocolor coded DSM.



Figure 9. Building detection for “Victoire boulevard” site.

Test site	Error I (%)	Error II (%)	Total Error (TE) in %	Mention
Hermann	0.22	0.01	0.01	Excellent (TE<1%)
Victoire boulevard	1.57	0.34	0.55	Excellent (TE<1%)
Strasbourg centre	1.46	0.97	1.12	Very good (1<TE<5%)

Table 10: Precision of building/not-building segmentation

At last, more independent quantitative evaluation consists in counting the detected buildings among the existing buildings. Table 11 proves that the detection rate is very satisfying and validates definitely our method.

Test site	Number of detected buildings	Number of non detected buildings	Total number of buildings	Detection rate (%)
Hermann	15	0	15	100
Victoire boulevard	60	4	64	94
Strasbourg center	64	3	67	95

Table 11: Rate of correctly detected buildings.

Nevertheless, this approach shows limitations in three main aspects. On the one hand, the classification precision is function of the point density and decreases with it. On the other hand, when trees and buildings are simultaneously close to each other and of the same height, the distinction becomes difficult. Furthermore, if a bloc of buildings is composed of several buildings with similar heights (falling under the threshold  $S_1$ ) the algorithm will misclassify the “off-terrain” pixels as “terrain”. So, the use of shape or geometric criterions has to be considered. At last, a methodology leading to deduce the most appropriate threshold according to the urban typology has to be developed.

## 6. CONCLUSION

This paper presents a new approach for detecting buildings in a Lidar point cloud, using exclusively the first echo. The most relevant idea is to benefit from the original point locations at strategic moments of the segmentation. While eliminating automatically the misclassifications caused by terrain discontinuities, the developed algorithm takes advantage of the topology of points belonging to one cell and produces a building segmentation image with high accuracy. Thus, the Lidar data are considered on a point level, pixel level, segment level and global level during the processing chain. Nevertheless, this methodology needs to be improved since in particular cases, some small vegetation segments may remain at the end of the process. Further investigations should also allow to predefine the optimal threshold referring to the urban typology. At this stage, the reconstruction of the building geometry in the forthcoming modelling phase can be considered.

## REFERENCES

- Baltsavias, E., Gruen, A., Van Gool, L., 2001. (Editors): *Automatic Extraction of Man-Made Objects from Aerial and Space Images (III)*, A.A. Balkema Publishers, ISBN 9058092526, 415p.
- Elaksher, A. F., and Bethel, J. S., 2002. Reconstructing 3D buildings from Lidar data. *Int. Archives of Photogrammetry and Remote Sensing*, Vol. XXXIV, part 3A/B, ISSN 1682-1750, pp102-107.
- Elmqvist, M., 2001. Ground Estimation of Laser Radar Data using active shape Models. *OEEPE workshop on Airborne Laserscanning and Interferometric SAR for Detailed Digital Elevation Models*, Stockholm, Sweden.
- Kraus, K., and Pfeifer, N., 1998. Determination of terrain models in wooded areas with airborne laser scanner data. *ISPRS Journal of Photogrammetry and Remote Sensing*, 53, pp. 193–203.
- Lee, I, Schenk, T, 2002. Perceptual organization of 3d surface points. *Photogrammetric computer vision. ISPRS Commission III*, Graz, Austria. Vol. XXXIV, part 3A/B, ISSN 1682-1750.
- Lohmann, P., Koch, A., Schaeffer, M., 2000. Approaches to the filtering of laser scanner data. Vol. 33, *Int. Archives of Photogrammetry and Remote Sensing*, Amsterdam, pp. 540–547
- Lohmann, P., and Jacobsen, K., 2004. Filterung segmentierter Oberflächenmodelle aus Laserscannerdaten. In: *PFG* (2004), Nr. 4, S. 279-287.
- Maas, H.-G., 1999. The potential of height texture measures for the segmentation of airborne laserscanner data. *Proceedings of the 4<sup>th</sup> International Airborne Remote Sensing Conference*, Ottawa, Vol. I, pp. 154-161.
- Maas, H.-G., 2005. Akquisition von 3D-GIS Daten durch Flugzeuglaserscanning. *Kartographische Nachrichten*, Vol. 55, Heft 1, S. 3-11.
- Maas, H.-G., Vosselman, G., 1999. Two algorithms for extracting building models from raw laser altimetry data. *ISPRS Journal of Photogrammetry & Remote Sensing* Vol. 54, No. 2/3,
- Marmol, U., Jachimski, J., 2004. A FFT based method of filtering airborne laser scanner data. *Int. Archives of Photogrammetry and Remote Sensing*, ISSN 1682-1750, Vol. XXXV, part B3.
- Pfeifer, N., Reiter, T., Briese, C., Rieger, W., 1999. Interpolation of high quality ground models from laser scanner data in forested areas. *Joint Workshop of the ISPRS working groups III/5 and III/2*, La Jolla, CA, USA, Nov. 9 – 11 1999.
- Rottensteiner, F., Briese, Ch., 2002. A new method for bulding extraction urban areas from high-resolution LIDAR data. *Int. Archives of Photogrammetry and Remote Sensing*, Vol XXXIV / 3A (2002), ISSN 1682-1750; 295 - 301.
- Sithole, G., Vosselmann, G., 2003. Automatic Structure Detection in a Point-Cloud of an Urban Landscape, *2nd Joint Workshop on Remote Sensing and Data Fusion over Urban Areas (URBAN2003)*, May 22-23, Berlin, Germany.
- Sithole, G., 2001 . Filtering of laser altimetry data using a slope adaptative filter. *Int. Archives of Photogrammetry and Remote Sensing*, Annapolts, Vol. XXXIV – 3/W4
- Tóvári, D., Vögtle, T., 2004. Classification methods for 3D objects in laserscanning data. *Int. Archives of Photogrammetry and Remote Sensing*, ISSN 1682-1750, Vol. XXXV, part B3.
- Vosselman, G., 2000. Slope based filtering of laser altimetry data. Vol. XXXIII, *Int. Archives of Photogrammetry and Remote Sensing*, Amsterdam, pp. 935–942, Part B3.
- Vosselman, G. and Maas, H., 2004. Airborne Laser Altimetry: DEM production and Automatic Feature Extraction. *Tutorial TU6 held at the XX<sup>th</sup> ISPRS Congress* in Istanbul, July 14, 2004.
- Wang, M., Tseng, Y.-H., 2004. Lidar data segmentation and classification based on octree structure. *Int. Archives of Photogrammetry and Remote Sensing*, ISSN 1682-1750, Vol. XXXV, part B3.
- Weinacker, H., Koch, B., Heyder, U., Weinacker, R., 2004. Development of filtering, segmentation and modelling modules for LIDAR and multispectral data as a fundament of an automatic forest inventory system. *Int. Archives of Photogrammetry and Remote Sensing*. Freiburg, Germany, Volume XXXVI, Part 8/W2. ISSN 1682-1750.
- Wotruba, L., Morsdorf, F., Meier, E., Nüesch, N., 2005. Assessment of sensor characteristics of an airborne laser scanning using geometric reference targets. *Proceedings of the ISPRS Workshop Laser scanning 2005*. Enschede, The Netherlands, ISSN 1682-1777.
- Yu., X., Hyypä., H., Kaartinen., H., Hyypä., J., Ahokas., E., Kaasalainen., S. 2005. Applicability of first pulse derived digital terrain models for boreal forest studies factors affecting the quality of DTM generation in forested areas. *Proceedings of the ISPRS Workshop Laser scanning 2005*. Enschede, The Netherlands, ISSN 1682-1777.